

---

# Deep End-to-End Survival Analysis with Temporal Consistency

---

Mariana Vargas Vieyra\*  
EPFL  
mariana.vargas-vieyra@epfl.ch

Pascal Frossard  
EPFL  
pascal.frossard@epfl.ch

## Abstract

In this study, we present a novel Survival Analysis algorithm designed to efficiently handle large-scale longitudinal data. Our approach draws inspiration from Reinforcement Learning principles, particularly the Deep Q-Network paradigm, extending Temporal Learning concepts to Survival Regression. A central idea in our method is temporal consistency, a hypothesis that past and future outcomes in the data evolve smoothly over time. Our framework uniquely incorporates temporal consistency into large datasets by providing a stable training signal that captures long-term temporal relationships and ensures reliable updates. Additionally, the method supports arbitrarily complex architectures, enabling the modeling of intricate temporal dependencies, and allows for end-to-end training. Through numerous experiments we provide empirical evidence demonstrating our framework’s ability to exploit temporal consistency across datasets of varying sizes. Moreover, our algorithm outperforms benchmarks on datasets with long sequences, demonstrating its ability to capture long-term patterns. Finally, ablation studies show how our method enhances training stability.

## 1 Introduction

Survival Analysis (SA) [7] is a statistical framework concerned with the study of the time span from when a subject enrolls in a study to the time an event of interest occurs. Even though it has been widely used in the medical community [13] it can have numerous applications in other domains such as churn prediction [11, 23].

In the context of Survival Analysis we are presented with a dataset of observations, each of which is associated with a *survival time*. This type of data is referred to as *time-to-event* data. In the most common setting, the practitioner is tasked with regressing the life span of each subject within a fixed time window. It is not uncommon that, for certain subjects, no event is observed within the study period. These data points are called *right-censored*, or *censored* for short, and represent incomplete information about the event of interest. In the dynamic Survival Analysis setting we are presented with time series data rather than vector data. A common example is clinical trials, where daily health indicators are collected for patients. This longitudinal setting is arguably richer than the static one because we have information about the evolution of subjects through time. In this context, estimations of the survival status of the subjects are updated as new information becomes available, rather than relying on a snapshot of their condition.

Recently, a new approach to estimate survival models in dynamic settings has been proposed by Maystre and Russo [16]. Their algorithm, named Temporally Consistent Survival Regression (TCSR), introduces a discrete-time model that builds upon the intuition that elements in a given time-series dataset can be considered sequences of states drawn from a Markov chain. In this context, the event

---

\*Work done while at EPFL. Corresponding author, mail to: mariana.vargas-vieyra@mostly.ai

of interest is deemed as reaching a specific terminal state. The authors then leverage ideas from temporal-difference learning [25] to propose a method that hinges on the idea of temporal consistency. That is, reaching the terminal state in  $k$  steps when departing from some initial state is, on average, the same as reaching the terminal state in  $k - 1$  steps when departing from the following state. At each training step the algorithm queries the current model to obtain a set of "soft targets". These targets serve as the guiding signal to fit the model using the Maximum Likelihood Estimator (MLE). The authors empirically showed that TCSR outperforms baseline SA methods in small datasets, highlighting the benefits of incorporating temporal consistency into SA. However, we argue that TCSR suffers from three limitations that pose challenges in dealing with large datasets requiring batching or involving long sequences spanning extensive time windows. Firstly, TCSR requires a complete pass through the dataset to compute the soft targets, which can significantly slow down training when the dataset is large. Secondly, the model must be re-trained from scratch at each training step using the obtained soft targets. This makes it very challenging to process data in batches and impedes end-to-end training. Finally, TCSR updates these soft targets at each training step, leading to unstable training dynamics and introducing substantial variance in the estimations [18]. Despite the demonstrated benefits of bringing temporal consistency to Survival Analysis in small datasets [16], we argue that overcoming these limitations is crucial for the application of these ideas to large-scale datasets with potentially long sequences.

The main goal of this work is to address the scalability challenges that temporal consistency poses for Survival Analysis. Drawing inspiration from Deep Reinforcement Learning [18, 15, 19] we present a novel framework that brings temporal consistency to longitudinal data in large-scale scenarios where TCSR cannot be applied due to its limitations in handling long sequences and batch processing. We introduce a *target network* that mirrors the structure of the model's parameterizing network. The aim of the target network is to generate stable target signals for supervising the model's main network. Its introduction provides more control over the frequency of target updates. By keeping the targets fixed for longer periods, we do not only stabilize the learning process but also enable efficient handling of data in batches. Furthermore, the model's parameters can be fitted end-to-end, without requiring re-training at every target update. This capability permits to accommodate more expressive architectures that can better model intricate temporal patterns and long-term dependencies. Notably, our method can be easily incorporated into most survival algorithms by simply introducing a target network that mirrors the main model. We update the model's parameters using Stochastic Gradient Descent (SGD), and the target network using a slow moving average of the main network. Our experiments on large datasets requiring batch processing highlight the advantages of the temporal consistency guidance provided by our framework. Additionally, we empirically demonstrate its ability to stabilize training and reduce variability in the estimates. These results underscore the practical benefits of our approach, especially in real-world applications involving large-scale datasets or fine-grained measurements that yield extensive time-series data.

Our contributions can be summarized as follows:

- We introduce a novel framework that brings temporal consistency to large scale survival analysis problems, and that can be easily incorporated in most survival algorithms for longitudinal data.
- By leveraging a target network that acts as a delayed copy of the main model's parameters we are able to bootstrap "slow moving targets". This helps stabilizing training and facilitates batch processing of the data.
- Our algorithm can be trained in an end-to-end fashion, and can seamlessly incorporate expressive neural network architectures that can better capture complex temporal relationships in large sequences.
- Finally, we empirically show that our framework can effectively utilize temporal consistency in datasets of larger sizes, outperforming classical baselines<sup>2</sup>.

---

<sup>2</sup>Code: <https://anonymous.4open.science/r/survan-7F5D>

## 2 Related work

Broadly speaking, Survival Analysis methods can be classified into two groups according to whether they process static vector data or time-varying features. We call these static Survival Analysis and dynamic Survival Analysis respectively.

Among the static methods, many recent works leverage Deep Learning models. DeepSurv proposed by Katzman et al. [8] uses a proportional hazard Cox regression model parameterised by a neural network. The method introduced by Kvamme et al. [11] scales to large datasets and introduces an extension for training non-proportional hazard Cox models. Other approaches deviate from the Cox regression model. Lee et al. [12] consider discrete time steps and predict the probability of the event of interest occurring over the whole time line making no assumptions about the underlying stochastic process of the data. Ren et al. [23] alleviate the proportional hazards assumption by introducing a flexible architecture based on Recurrent Neural Networks. The method proposed by Nagpal et al. [22] models the conditional survival distribution of an individual as a mixture of fully parametric distributions. Recently, Wu et al. [29] introduced neural frailty machine framework to extend the proportional hazard assumption. Some authors propose to reformulate survival analysis to leverage different frameworks. For example, Vauvelle et al. [27] reframe the survival regression problem as a ranking problem.

Our work is situated within the dynamic Survival Analysis group, where there has been an increasing interest and significant advances. Recent works introduce neural network in the treatment of longitudinal data. For instance, Kvamme et al. [11] extend traditional models to non-proportional hazards by treating the time variable as a regular covariate, allowing for more flexibility in modeling survival outcomes. Nagpal et al. [21] builds upon the Deep Survival Machine [22] by adding time-dependant feature representations learned with a recurrent neural network. Taking a different perspective, Kim [9] leverages the Permenental Process framework to propose a non-parametric estimator of the hazard function. What these methods have in common is that they rely solely on the observed survival outcome as the supervising signal. Maystre and Russo [16] propose a method that deviates from this idea. Drawing inspiration from Temporal Difference Learning, they introduce Temporal Consistent Survival Regression (TCSR), an algorithm that combines the true survival outcomes from the dataset with the model’s internal knowledge. This combination allows for more robust parameter updates, leveraging the model’s understanding of the temporal dynamics involved. Our approach exploits this idea as well, effectively bringing temporal consistency to large-scale scenarios where TCSR faces scalability limitations.

## 3 Preliminaries

In this Section we introduce foundational concepts that are relevant to our method. More specifically, we discuss dynamic Survival Analysis, its formulation as a classification problem, and how temporal consistency can improve survival models in terms of robustness and accuracy.

### 3.1 Dynamic Survival Analysis

Following the formulation proposed by Maystre and Russo [16] we consider finite sequences of the form  $(x_0, \dots, x_{t-1})$  of length  $t$  to be drawn from a Markov chain with state space  $\mathcal{X}$  and transition probabilities  $p(x'|x)$ . This assumption allows us to reason about the causality of the data and to leverage temporal consistency<sup>3</sup>. These sequences eventually reach a *terminal state* denoted  $\emptyset$ , which is absorbing. The goal of Survival Analysis in this context is to model the time lapse  $T$  between the initial state  $x_0$  and the event  $x_i = \emptyset$  for some  $i$ . The random variable  $T$ , often referred to as *time-to-event*, represents the time at which the event of interest occurs.

Let

$$F(k|x) = p(T \leq k|x_0 = x) \quad \text{and} \quad f(k|x) = p(T = k|x_0 = x)$$

be the distribution function and probability mass function of  $T$  respectively, provided the initial state is  $x$ . Then we can define two crucial quantities that characterise the survival distribution of  $T$ . The

---

<sup>3</sup>The Markovian assumption need not be restrictive: depending on the application, states can be formulated to represent the entire past up to that moment.

*survival function*  $S(k|x)$  describes the probability of a sequence starting at state  $x$  and *surviving* past a certain time  $k$ . The *hazard function*  $h(k|x)$  represents the risk of a sequence reaching its terminal state at time  $k$ , provided it departed from the initial state  $x$  and that the event of interest has not yet been observed. They are defined as

$$S(k|x) = 1 - F(k|x) \quad \text{and} \quad h(k|x) = p(T = k|T \geq k, x_0 = x)$$

respectively.

A very popular choice for modeling survival data is to fit a parametric or semi-parametric form of the hazard function to the observed data,

$$\text{logit}(h_\theta(k|x)) = g_\theta(x, k). \quad (1)$$

A widely used example of this formulation is the proportional hazards Cox regression model [5] where  $g_\theta(x, k) = h_0(k) + \tilde{g}_\theta(x)$ . Here,  $h_0$  is a *baseline hazard* that depends only on the time and  $\tilde{g}_\theta$  is a relative risk function that depends only on the covariates. When handling a discrete time domain one can use the discrete Cox model [2]. In this case the baseline hazard can be treated as a constant or a separate vector of parameters. Recent literature has expanded this model to incorporate more expressive architectures while keeping the proportional assumption [8], or alternatively, deviating from it by introducing a non-proportional formulation [11]. Furthermore, one can deviate from the Cox model and parameterise Equation (1) directly with a neural network [22, 23].

### 3.2 Maximum Likelihood Estimation

The general practice is to collect a dataset with sequences sampled from the Markov chain, each up to a maximum length or *horizon*, denoted  $H$ . For some sequences the event of interest is not observed, meaning they do not reach the terminal state. These sequences are referred to as *censored*. Let  $\mathbf{1}\{\cdot\}$  be an indicator function that returns 1 if the condition inside the brackets is true and 0 otherwise. Given a sequence  $x = (x_0, \dots, x_{t-1})$  of length  $t$ , we define a *censoring indicator* as  $c = \mathbf{1}\{x_{t-1} \neq \emptyset\}$ , indicating whether  $x$  has reached the terminal state within  $t$  steps. Given a dataset  $\mathcal{D} = \{(x^{(i)}, t^{(i)}, c^{(i)})\}_{i=1}^n$ , where  $x^{(i)} = (x_0^{(i)}, \dots, x_{t^{(i)}-1}^{(i)})$  is a sequence,  $t^{(i)}$  its duration, and  $c^{(i)} = \mathbf{1}\{x_{t-1} \neq \emptyset\}$  is the censoring indicator, we can frame the survival regression problem as a classification problem [12, 6]. We can then express the Maximum Likelihood Estimator (MLE) as follows

$$\theta^* \in \arg \min_{\theta} \sum_{i=1}^n \sum_{k=0}^{t^{(i)}-1} \sum_{\ell=0}^{k-1} w_{k-\ell}^{(i)} \text{CE}(y_{k-\ell}^{(i)}, h_\theta(k-\ell|x_\ell^{(i)})). \quad (2)$$

Here, CE is the binary cross-entropy loss and  $w_k^{(i)} = \mathbf{1}\{t^{(i)} < k\}$  is a variable that indicates whether the  $i^{\text{th}}$  sequence is still active at time  $k$ . The event indicator is defined as  $y_k^{(i)} = \mathbf{1}\{t^{(i)} - 1 = k \wedge c^{(i)} = 0\}$ , and indicates whether an uncensored sequence reached the terminal state. In the dynamic Survival Analysis framework one might fix  $\ell = 0$ . In that case the MLE is based on predictions made when departing from the first state, thus fully disregarding intermediate states. Letting  $\ell$  take values larger than zero is an extension called *landmarking* that overcomes this limitation by also regressing the hazard rate of intermediate states [3].

### 3.3 Temporal Consistency in Survival Analysis

Maystre and Russo [16] introduce Temporally Consistent Survival Regression (TCSR), a method that hinges on the notion of temporal consistency. The rationale behind this idea is that if we reach the terminal state in  $k$  steps when departing from some state  $x$ , then, on average, that should be equivalent to departing from the next state, and reaching the terminal state after  $k-1$  steps. Temporal consistency makes for a more robust model with respect to noise and helps avoiding overfitting by better capturing the patterns of time-indexed data. This idea is formally stated in the following identities:

$$f(k|x) = E_{x' \sim p(\cdot|x)}[f(k-1|x')] \quad \text{and} \quad S(k|x) = E_{x' \sim p(\cdot|x)}[S(k-1|x')], \quad (3)$$

where  $p(\cdot|x)$  is the transition distribution.

In a nutshell, the TCSR algorithm works by bootstrapping predictions at the next step from the model’s current parameters. These predictions are used as pseudo-targets for updating the model’s parameters. A limitation of this approach is that it requires a complete pass through the dataset to compute these soft targets, which can significantly slow down training on large datasets. Additionally, the model must be re-trained from scratch at each step using the updated soft targets, which makes it difficult to process data in batches or perform end-to-end training. The frequent updates of the soft targets also introduce variance in the estimations, leading to unstable training dynamics.

In the original paper, the model’s updates are performed using Newton’s optimization method at each iteration. The authors prove that the TCSR algorithm is equivalent to a fixed-point iteration problem with the empirical Markov chain and transition probabilities. They also provide a generalization of this algorithm, TCSR( $\lambda$ ), where they introduce the hyperparameter  $\lambda$  to control the trade-off between bootstrapping near-term predictions and learning ground truth events from the distant future.

In the following Section we build upon these ideas and provide a mechanism to bring temporal consistency to survival problems involving large datasets with sequences of potentially large horizons.

## 4 Proposed Method

In this section, we introduce Deep Temporally Consistent Survival Regression (DeepTCSR), a novel method designed to extend the benefits of temporal consistency to real-world applications involving large datasets and long sequences. While TCSR was the first method to incorporate temporal consistency in Survival Analysis, it suffers from significant limitations that make it impractical for large-scale data. In contrast, our approach not only scales up by allowing efficient batch processing of data, but also enables end-to-end training.

One of the key innovations in DeepTCSR is the introduction of a target network that mirrors the main network, a mechanism inspired by Deep Q-Networks (DQN) [17]. The target network plays a crucial role by bootstrapping knowledge from the current model, generating "soft" targets that guide the learning process. At its core, our method decouples parameter updates from the immediate predictions, stabilizing training and reducing variance. By fixing the soft targets for multiple iterations, we not only mitigate the instability caused by frequent target updates in TCSR but also improve the model’s convergence. Also, this design allows us to seamlessly utilise expressive architectures, such as deep neural networks, and train the model end-to-end. As a result, DeepTCSR not only preserves the strengths of temporal consistency but also addresses the scalability and stability issues of TCSR, making it applicable to real-world, large-scale datasets.

### 4.1 Scalable Survival Regression with Temporal Consistency

We consider practical settings where we have access to a dataset of sequences of varying length as described in Section 3. Our architecture has two main components, a *main network* and a *target network*. The main network is used to parameterize the hazard function in Equation (1), and it has a vector of parameters denoted as  $\theta$ . This is the network that will be employed at inference time to calculate the hazard rates using the function  $h_\theta$ . We also introduce a target network parameterized by  $\varphi$  that serves as a delayed copy of the main network. The purpose of the target network is to provide a stable signal for the main network to be updated. Throughout the training process, given a sequence  $x$  with  $t$  states<sup>4</sup> and censoring indicator  $c$ , we use the target network to bootstrap target hazards  $h_\varphi(k|x_\ell)$  and weights  $S_\varphi(k|x_\ell)$  for  $k = 0, \dots, t - 1$  and  $\ell = 0, \dots, t - 1$ , based on the current model estimate. These values can be considered the "soft" targets and weights, corresponding to the "hard" value indicators  $y_k$  and  $w_k$  in Equation (2). The supervisory signal is then obtained by interpolating the true "hard" value indicators  $y_k$  and  $w_k$  from the dataset with the "soft" targets  $h_\varphi(k|x_\ell)$  and weights  $S_\varphi(k|x_\ell)$  bootstrapped from the model’s target network. We call these the *pseudo-targets* and *pseudo-weights* respectively. Only the main network is updated using gradient descent, while the target network is updated via an exponential moving average to remain close to the main network.

**Pseudo-target and pseudo-weight coefficients.** We supervise the model with pseudo-targets  $\tilde{y}_{k,\ell}$  and pseudo-weights  $\tilde{w}_{k,\ell}$  obtained through recursive formulas. The pseudo-targets are computed as

<sup>4</sup>In this context, one can also say that the sequence  $x$  has a duration of  $t$  time steps.

---

**Algorithm 1** DeepTCSR Algorithm

---

**Inputs:** Data  $\mathcal{D}$ , init.  $\theta, \lambda \in [0, 1]$ 

- 1: Initialize  $\varphi \leftarrow \theta$
  - 2: **repeat**
  - 3:   Sample sequence  $x$
  - 4:   Compute  $h_\varphi(k|x_\ell)$  for  $k, \ell = 0, \dots, t$
  - 5:   Obtain targets  $\tilde{y}_{k,\ell}$  and weights  $\tilde{w}_{k,\ell}$  using Equations (4) and (5) resp.
  - 6:   Update  $\theta$  with SGD by minimizing Eq (6).
  - 7:   Update  $\varphi$  with moving average
  - 8: **until** max iterations
- 

follows:

$$\tilde{y}_{k,\ell} = \lambda \tilde{y}_{k-1,\ell+1} + (1 - \lambda) h_\varphi(k - 1|\ell + 1), \quad (4)$$

where  $k, \ell = 0, \dots, t - 1, k \leq \ell$ . The initialization of the pseudo-targets is done as follows: at the first time step,  $k = 0$ , we initialize  $\tilde{y}_{0,\ell} = 0$  because all sequences are considered active, that is, the event of interest is not observed at  $k = 0$ . Additionally, when departing from the terminal state,  $\ell = t - 1$ , the pseudo-target is fixed as the true label from the dataset, i.e.,  $\tilde{y}_{k,t-1} = y_{t-1}$ . Using analogous reasoning we derive the recursive formula for the pseudo-weights as follows:

$$\tilde{w}_{k,\ell} = \lambda \tilde{w}_{k-1,\ell+1} + (1 - \lambda) S_\varphi(k - 1|\ell + 1), \quad (5)$$

where  $\tilde{w}_{0,\ell} = 1, \tilde{w}_{k,t-1} = S_\varphi(k - 1|t - 1)$  if  $c = 1$  and  $\tilde{w}_{k,t-1} = w_{t-1}$  if  $c = 0$ .

Intuitively, the equations above compute the pseudo-targets by combining the soft targets and weights bootstrapped from the target network with the "hard" true label indicators and true weight indicators, respectively from the dataset, with the hyperparameter  $\lambda$  controlling the trade-off between the two. When  $\lambda = 0$  we only use the soft targets and weights to fit the model. This implies that we are only taking into account the next state. In contrast, setting  $\lambda = 1$  is equivalent to the SA baseline with landmarking [3].

**Training.** To fit the model's main parameterizing network we minimize the weighted Cross Entropy loss between the model's estimates and the pseudo-targets. The loss function is

$$\mathcal{L}(\theta) = \sum_{i=1}^n \sum_{k=0}^{t^{(i)}-1} \sum_{\ell=0}^{k-1} \tilde{w}_{k,\ell}^{(i)} \text{CE}(\tilde{y}_{k,\ell}^{(i)}, h_\theta(k - \ell|x_\ell^{(i)})). \quad (6)$$

Note that this objective is a weighted MLE with pseudo-targets and weights obtained through Equations (4) and (5).

We update the main network parameterized by  $\theta$  with Stochastic Gradient Descent (SGD). The target network parameterized by  $\varphi$  is updated with an exponential moving average formula as  $\varphi = \tau\theta + (1 - \tau)\varphi$ , where  $\tau \in (0, 1)$  acts as a target learning rate and is typically close to 0. This ensures the target network will remain close to the main network during training. Intuitively, a larger value of  $\tau$  implies more frequent updates of the target network and hence introduces more variance in the estimations.

The learning procedure is described in Algorithm 1.

## 4.2 Connection to TCSR and DQN

In Reinforcement Learning, Temporal Difference learning with  $\lambda$  return (TD( $\lambda$ )) [25] is a learning algorithm that aims at estimating a scalar-valued function that represents the expected reward based on accumulated experiences over time. The  $\lambda$  coefficient captures a sense of memory over a time window. Intuitively, we update our estimates by taking into account a certain range of future events. When  $\lambda$  is closer to 0 we privilege more recent events, in contrast, when  $\lambda$  approaches 1, we place greater emphasis on events that occurred further in the future. TCSR and DeepTCSR utilize TD( $\lambda$ ) as a foundation, exploiting the consistency assumption described by Equations (3).

On the other hand, Q-Learning [28] is a particular instance of TD learning where the goal is to estimate a scalar function that maximizes the expected return of all possible transitions when departing from a

specific initial state. The Deep Q-Network (DQN) algorithm [17] combines Q-learning with deep neural networks in order to handle large-scale state spaces and leverage complex model architectures. It employs a technique called experience replay, which consists of storing past transitions in memory. These transitions are sampled randomly during training, providing a diverse set of experiences for the network to learn from. Experience replay is a form of using past temporal differences to update the model. To stabilize training, DQN introduces a target network that essentially is a delayed copy of the main Q-network. This target network is used to generate target values for training the model. In other words, the model is supervised with soft labels or "slow moving labels".

In the same way that DQN brought deep learning and scalable solutions to Q-learning, our approach extends TCSR by making temporal consistency applicable to large datasets. Instead of directly updating from observed outcomes at every step, we compute soft targets using the target network, which provides a more consistent and robust signal for parameter updates. This is analogous to how DQN uses experience replay’s past transitions to ensure more stable updates. Unlike TCSR, which recalculates pseudo-targets at every iteration, our method stabilizes training by controlling the update frequency of the target network through the  $\tau$  hyperparameter. This separation of the target network from the main model also enables end-to-end training, allowing us to leverage more expressive neural architectures to model complex temporal patterns. By addressing TCSR’s limitations, our method expands the use of temporal consistency to a broader range of real-world applications involving large datasets.

## 5 Experiments

The goal of our experimental study is twofold. On the one hand, we aim to empirically verify that we perform comparably to the TCSR method proposed by Maystre and Russo [16] when using small datasets and linear models. On the other hand, we intend to empirically assess the benefits of our framework in mid and large-scale datasets that necessitate batch processing and can benefit from more expressive model architectures.

We present results for small survival datasets as well as for larger churn prediction datasets, real-world and synthetic. We evaluate the quality of our method using two standard metrics for Survival Analysis: the Concordance Index (CI) and the Integrated Brier Score (IBS). Further details on these metrics can be found in Appendix D.1. Additionally, we elucidate the issue of biased hazard estimates, a common phenomenon in survival models that is exacerbated when leveraging temporal consistency. We argue that while this bias can negatively impact the model’s performance in terms of the Integrated Brier Score, it does not compromise the model’s ability to correctly rank survival outcomes. Finally, we examine the stabilizing capabilities introduced by the target network, particularly in terms of reducing the variability of the estimates.

### 5.1 Small datasets

The goal of these initial experiments is to assess the performance of our DeepTCSR algorithm in comparison with the approach introduced by Maystre and Russo [16]. Specifically, we aim to confirm that our method yields similar results to theirs. Following a similar experimental setup as the one outlined in their work, we employ a linear model of the form

$$\text{logit}[h_{\theta}(k|x)] = \beta^T x + \alpha_k$$

with learnable parameters  $\theta = (\alpha, \beta)$ , for all models. We conduct experiments on two real-world datasets and one synthetic dataset.

The two real-world datasets come from the medical domain and follow the survival status of patients participating in a specific clinical trial. Both combine static features and time-varying features. In this context, the time-varying or "dynamic" features are biomarkers that are measured periodically within a time window of many years. For our experiments we only considered events occurring at discrete time points, thus disregarding the potentially different time intervals between each pair of measurements. The first dataset, PBC2, follows 312 patients suffering from a liver disease called Primary Biliary Cirrhosis [20]. The second dataset, AIDS, contains information of 467 patients diagnosed with HIV/AIDS [1]. We finally consider a synthetic dataset where we generated sequences using a 20-dimensional Gaussian random walk (SmallRW) with the horizon set to 11. At each step  $k$

we emulated a churn event as follows: the sequence finishes with probability  $p = \sigma(a^\top x_k + b)$  where  $a \in \mathbb{R}^{20}$  and  $b \in \mathbb{R}$  are user-input hyperparameters.

We compare the TCSR and DeepTCSR with two baselines consisting on regular Survival Analysis without landmarking (SA Init State) and with landmarking (SA Landmarking). For both TCSR and DeepTCSR we fix  $\lambda = 0$ . We split the dataset using 5-fold cross validation and fit the models using training sets with size in  $\{10, 20, 30, 50, 75, 100\}$ . For both baseline methods and TCSR we used the hyperparameters reported Maystre and Russo [16] in the original paper. The authors performed a grid search across various regularization coefficients for each dataset, each method, and each evaluation metric. For our method we did not perform any hyperparameter search but rather fixed the main hyperparameters. For PCB2 and SmallRW we fix the weight decay regularization hyperparameter to 0.0, whereas for AIDS we fixed it to 0.4. We set the target learning rate  $\tau = 0.1$  and the SGD learning rate to 0.1, and we fit the model during 100 epochs for all datasets with Adam optimizer [10]. Results on average CI and IBS values across five random splits are summarized in Figure 1.

We observe that in general SA without landmarking is the worst performing model and that methods based on temporal consistency, TCSR and DeepTCSR, outperform both benchmarks. This difference in performance becomes smaller as the training size increases. Furthermore, we verify that our method is on a par with TCSR in most cases. Surprisingly, for PCB2 and, to a lesser extent, AIDS, we tend to perform better than TCSR in smaller datasets, without grid search. This difference is more pronounced in terms of CI. Finally, we note that the advantages in using Landmarking, TCSR and DeepTCSR in the AIDS dataset is less evident. We argue that this is due to the fact that this dataset has a very small horizon and hence it benefits less from variance-reducing algorithms. Furthermore, this dataset has a single time-varying covariate, and it is likely that static features are informative enough of the survival outcome of patients.

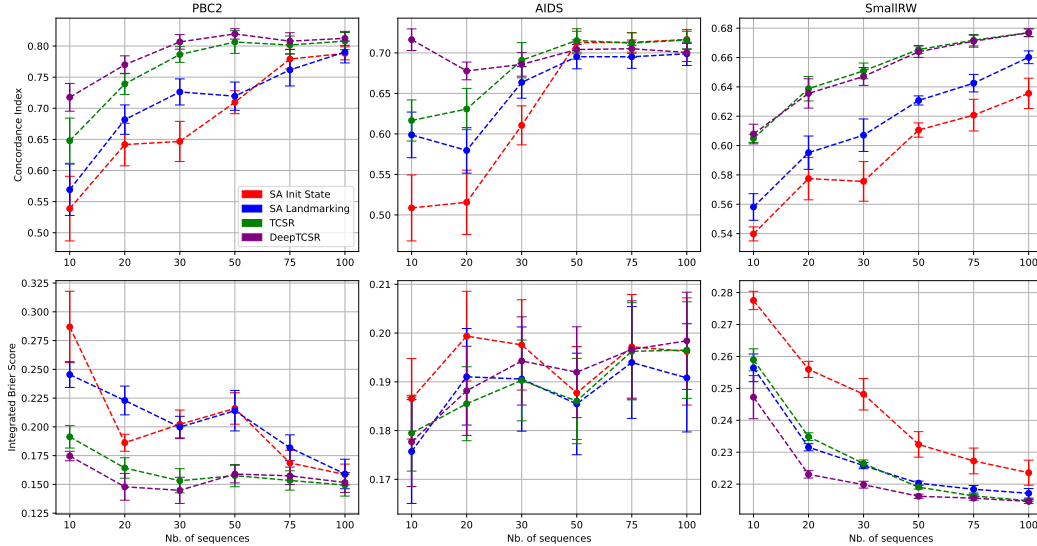


Figure 1: Performance of event prediction in small datasets. We present results in terms of the CI (higher is better) and IBS (lower is better). The error bars represent the mean and standard deviation over five random seeds.

## 5.2 Large datasets

We also conduct experiments on larger datasets that require batch processing due to their large size or extended horizon. Datasets with larger horizons can benefit from more complex model architectures that better capture long-term time dependencies. For this reason, in this Section we compare our method, DTCSR with values of  $\lambda \in \{0.0, 0.9, 0.95\}$  against the baselines. We choose these values of  $\lambda$  to explore both scenarios: one where near-term events are prioritized ( $\lambda = 0$ ) and another where longer-range look-aheads are considered ( $\lambda = 0.9, 0.95$ ). We do not include TCSR in these experiments as it does not effectively scale to larger datasets, making it unsuitable for comparison in this context.



Our first dataset is LastFM, a churn prediction dataset [4]. Churn prediction is the task of detecting which costumers are likely to stop using a service. Provided a set of user features or logs associated with "churning times", it is fairly straightforward to formulate churn prediction as a survival problem. LastFM contains the listening history of almost 1000 users between 2004 and 2009 in a popular music streaming platform. The dataset contains information from two distinct sources: one providing static features and the other offering time-varying covariates. Specific details about the times when users discontinued the service are also included. Users who did not withdraw from the platform are considered as censored. That is, the event of interest (churning) was not observed. In this work we focus exclusively on the time-varying features, which consists of time-stamped logs that specify which artist and song the user is listening to. We use the artist and song IDs as features, and utilize a base-N categorical encoder to encode each identifier. Because of the granularity of the time measurements this dataset varies a lot in terms of sequence length. Users can accumulate tens of thousands of entries while others may have as few as two. As a result, the dataset is very sparse. To overcome this issue we employ two per-user aggregation strategies. The first one consists in taking the last song and artist the user listened to in each month of platform activity (MonLastFM). This yields sequences with a maximum length of 53. The second strategy employs daily aggregation, where we average features corresponding to all the songs and artists within each day (DayLastFM). This aggregation results in sequences of a maximum length of 1457. To reduce memory complexity, we partition the DayLastFM sequences into chunks, each with a length of 100.

We also include a dataset collected by [24] consisting of simulated measurements from aircraft engines that run until failure. It provides time-series measurements of several engine parameters overtime, allowing for the analysis of the engine degradation process. In this context, the event of interest is engine failure, and censored sequences correspond to engines that did not fail during the study period. Approximately 50% of the sequences are censored, and the dataset has an average horizon of 168 time steps, with some extending beyond 300 time steps, making it a large horizon dataset.

In the current literature the availability of mid and large scale survival datasets is very limited. While in general we can find large datasets in the context of static SA, the scarcity of datasets is particularly pronounced in the context of time-varying settings. For this reason we complete this experimental section with a large-scale synthetic dataset (LargeRW). We used a Gaussian random walk model as in Section 5.1 with 50 features and a horizon  $H = 100$ . We generated 10000 samples with about 20% of censored sequences. Table 3 in Appendix C presents summary statistics for all datasets.

We compare DeepTCSR with  $\lambda \in \{0.0, 0.9, 0.95\}$  (DTCSR(0.0), DTCSR(0.9) and DTCSR(0.95)) to the SA baselines with and without landmarking. We parameterize all the models with a single-layer Transformer network [26]. We fixed the hidden size to 16 for all datasets and the target learning rate  $\tau = 0.01$ . For all datasets we used a batch size of 128, except for NASA where we set the batch size to 32 due to its large horizon. We randomly separated 80% of the elements as training set and left the rest as test set. For all datasets, we trained all the models for 100 epochs. We optimized all models with the Adam optimizer [10] with a weight decay fixed to 0.0001.

Results are summarized in Table 1. We highlight in bold those results that are significantly better based on a t-test with significance level  $\alpha = 0.05$  over eleven randomized experiments. In terms of CI we outperform the baselines in three datasets by a significant margin. Notably, when landmarking (SA Landmarking) improves over the baseline that uses only the initial state (SA Init State), DeepTCSR yields the best results with a larger value of  $\lambda$ . We also observe that in the LargeRW dataset, the best score is achieved with  $\lambda = 0.0$ . This is likely due to the fact that LargeRW was simulated using a Markov Gaussian process, where current events depend only on the immediate past, making a longer lookahead unnecessary for improving performance. In terms of IBS we outperform the baselines in MonLastFM and in NASA datasets, while remaining on a par with SA Landmarking in DayLastFM and LargeRW.

### 5.3 Effect of $\tau$ on the variability of the estimates

The stabilizing capabilities of introducing a target network have been widely studied and demonstrated in the context of Deep Reinforcement Learning [19, 15, 14]. In these studies, target networks help reduce variance and stabilize training by providing consistent target values.

Table 1: Performance of event prediction in big datasets. Following the same assessment as before, we report the mean and standard deviation over eleven random seeds for the CI (higher is better) and IBS (lower is better) scores.

Dataset	Method	CI Mean ( $\pm$ Std) $\uparrow$	IBS Mean ( $\pm$ Std) $\downarrow$
DayLastFM	SA Init State	0.976 ( $\pm$ 0.005)	0.054 ( $\pm$ 0.029)
	SA Landmarking	0.973 ( $\pm$ 0.008)	<b>0.010 (<math>\pm</math>0.006)</b>
	DTCSR(0.95)	0.977 ( $\pm$ 0.009)	<b>0.011 (<math>\pm</math>0.009)</b>
	DTCSR(0.9)	0.978 ( $\pm$ 0.006)	0.018 ( $\pm$ 0.008)
	DTCSR(0.0)	0.973 ( $\pm$ 0.008)	0.038 ( $\pm$ 0.012)
MonLastFM	SA Init State	0.816 ( $\pm$ 0.041)	0.136 ( $\pm$ 0.049)
	SA Landmarking	0.739 ( $\pm$ 0.071)	0.120 ( $\pm$ 0.034)
	DTCSR(0.95)	0.710 ( $\pm$ 0.057)	<b>0.082 (<math>\pm</math>0.016)</b>
	DTCSR(0.9)	0.805 ( $\pm$ 0.038)	<b>0.085 (<math>\pm</math>0.016)</b>
	DTCSR(0.0)	<b>0.860 (<math>\pm</math>0.017)</b>	0.106 ( $\pm$ 0.006)
NASA	SA Init State	0.461 ( $\pm$ 0.089)	0.306 ( $\pm$ 0.066)
	SA Landmarking	0.638 ( $\pm$ 0.043)	0.135 ( $\pm$ 0.020)
	DTCSR(0.95)	<b>0.730 (<math>\pm</math>0.109)</b>	<b>0.092 (<math>\pm</math>0.032)</b>
	DTCSR(0.9)	<b>0.715 (<math>\pm</math>0.097)</b>	<b>0.101 (<math>\pm</math>0.024)</b>
	DTCSR(0.0)	0.474 ( $\pm$ 0.071)	0.503 ( $\pm$ 0.047)
LargeRW	SA Init State	0.910 ( $\pm$ 0.055)	<b>0.032 (<math>\pm</math>0.004)</b>
	SA Landmarking	0.748 ( $\pm$ 0.045)	<b>0.027 (<math>\pm</math>0.011)</b>
	DTCSR(0.95)	0.916 ( $\pm$ 0.019)	<b>0.027 (<math>\pm</math>0.009)</b>
	DTCSR(0.9)	0.934 ( $\pm$ 0.010)	<b>0.031 (<math>\pm</math>0.006)</b>
	DTCSR(0.0)	<b>0.948 (<math>\pm</math>0.010)</b>	0.065 ( $\pm$ 0.006)

To explore the impact of our method in the variability of the estimates in the context of Survival Analysis we perform an ablation study on the target learning rate  $\tau$ . In Appendix A we present empirical evidence showing how the variability of the estimated hazard probabilities is reduced for smaller values of  $\tau$ . In addition to stabilizing training, our framework demonstrates improved performance in terms of CI and IBS for datasets with both small and large horizons. These results underscore the advantageous impact of leveraging smaller  $\tau$  values within our framework.

## 6 Conclusion

In this study, we introduced a novel framework for Survival Analysis, designed to efficiently handle time-to-event data with time-varying covariates in large-scale settings. Drawing inspiration from the Deep Q-Network (DQN) algorithm, our approach introduces a target network that provides a more stable training signal. This ensures temporal consistency while enabling mini-batch updates and end-to-end training. We argue that our method enables practitioners to exploit temporal consistency and effectively manage large datasets with long sequences. Furthermore, we can control the frequency of the training signal updates through the target learning rate hyperparameter  $\tau$ . Our ablation study on  $\tau$  demonstrates that this control leads to less variability on the estimated hazard rates and better performance in terms of popular metrics used to assess survival models, namely the Concordance Index and Integrated Brier Score.

We argue that the ability to seamlessly integrate complex architectures opens new opportunities for applying our framework beyond traditional small-scale datasets. This flexibility makes our approach particularly well-suited for diverse, real-world applications. For instance, in churn prediction, where datasets may contain information on thousands of users, or in resource allocation for cloud services, where decisions on memory allocation rely on fine-grained hardware logs spanning long longitudinal sequences. Exploring such avenues could lead to novel insights and expanded use cases for our framework across various domains.

## Acknowledgements

We would like to thank Pierre Ménard for his valuable feedback.

## References

- [1] Donald I Abrams, Alma I Goldman, Carolyn Launer, Joyce A Korvick, James D Neaton, Lawrence R Crane, Michael Grodesky, Susan Wakefield, Kathleen Muth, Stephen Kornegay, et al. A comparative trial of didanosine or zalcitabine after treatment with zidovudine in patients with human immunodeficiency virus infection. *New England Journal of Medicine*, 330(10): 657–662, 1994.
- [2] Paul D. Allison. Discrete-time methods for the analysis of event histories. *Sociological Methodology*, 13:61–98, 1982.
- [3] P. K. Andersen and N. Keiding. Multi-state models for event history analysis. *Statistical Methods in Medical Research*, 11(2):91–115, 2002.
- [4] Thierry Bertin-Mahieux, Daniel P.W. Ellis, Brian Whitman, and Paul Lamere. The million song dataset. In *Proceedings of the 12th International Conference on Music Information Retrieval (ISMIR 2011)*, 2011.
- [5] D. R. Cox. Regression models and life-tables. *Journal of the Royal Statistical Society: Series B (Methodological)*, 34(2):187–220, 1972.
- [6] Erin Craig, Chenyang Zhong, and Robert Tibshirani. Survival stacking: casting survival analysis as a classification problem, 2021.
- [7] John D Kalbfleisch and Ross L Prentice. *The Statistical Analysis of Failure Time Data*. John Wiley & Sons, 2nd edition, 2002.
- [8] Jared L Katzman, Uri Shaham, Alexander Cloninger, et al. Deepsurv: personalized treatment recommender system using a cox proportional hazards deep neural network. *BMC Medical Research Methodology*, 18(1):24, 2018. doi: 10.1186/s12874-018-0482-1.
- [9] Hideaki Kim. Survival permanental processes for survival analysis with time-varying covariates. In *Thirty-seventh Conference on Neural Information Processing Systems*, 2023. URL <https://openreview.net/forum?id=CYCzfXn6cZ>.
- [10] Diederik P Kingma and Jimmy Ba. Adam: A method for stochastic optimization. *arXiv preprint arXiv:1412.6980*, 2014.
- [11] Håvard Kvamme, Ørnulf Borgan, and Ida Scheel. Time-to-event prediction with neural networks and cox regression. *Journal of Machine Learning Research*, 20:129:1–129:30, 2019. URL <https://api.semanticscholar.org/CorpusID:195767074>.
- [12] Changhee Lee, William R. Zame, Jinsung Yoon, and Mihaela van der Schaar. Deephit: A deep learning approach to survival analysis with competing risks. In *Proceedings of the AAAI Conference on Artificial Intelligence (AAAI)*, 2018.
- [13] Elisa T Lee and Orlando T Go. Survival analysis in public health research. *Annual Review of Public Health*, 18:105–134, 1997. doi: 10.1146/annurev.publhealth.18.1.105.
- [14] Yitao Liang, Marlos C. Machado, Erik Talvitie, and Michael Bowling. Categorical deep q-networks. In *Proceedings of the AAAI Conference on Artificial Intelligence*, volume 32, 2018. doi: 10.1609/aaai.v32i1.11757. URL <https://ojs.aaai.org/index.php/AAAI/article/view/11757>.
- [15] Timothy P. Lillicrap, Jonathan J. Hunt, Alexander Pritzel, Nicolas Heess, Tom Erez, Yuval Tassa, ..., and Daan Wierstra. Continuous control with deep reinforcement learning. *arXiv preprint arXiv:1509.02971*, 2016.

- [16] Lucas Maystre and Daniel Russo. Temporally-consistent survival analysis. In *Neural Information Processing Systems*, 2022. URL <https://api.semanticscholar.org/CorpusID:258509685>.
- [17] Volodymyr Mnih, Koray Kavukcuoglu, David Silver, Alex Graves, Ioannis Antonoglou, Daan Wierstra, and Martin Riedmiller. Playing atari with deep reinforcement learning. 2013. URL <http://arxiv.org/abs/1312.5602>. cite arxiv:1312.5602Comment: NIPS Deep Learning Workshop 2013.
- [18] Volodymyr Mnih, Koray Kavukcuoglu, David Silver, Andrei A Rusu, Joel Veness, Marc G Bellemare, Alex Graves, Martin Riedmiller, Andreas K Fidjeland, Georg Ostrovski, et al. Playing atari with deep reinforcement learning. *arXiv preprint arXiv:1312.5602*, 2013.
- [19] Volodymyr Mnih, Koray Kavukcuoglu, David Silver, and et al. Human-level control through deep reinforcement learning. *Nature*, 518(7540):529–533, 2015.
- [20] Paul A Murtaugh, Elizabeth R Dickson, Greet M Van Dam, Michael Malinchoc, Patricia M Grambsch, Anne L Langworthy, and Charles H Gips. Primary biliary cirrhosis: prediction of short-term survival based on repeated patient visits. *Hepatology*, 20(1 Pt 1):126–134, Jul 1994. doi: 10.1016/0270-9139(94)90144-9.
- [21] Chirag Nagpal, Vincent Jeanselme, and Artur Dubrawski. Deep parametric time-to-event regression with time-varying covariates. In Russell Greiner, Neeraj Kumar, Thomas Alexander Gerdts, and Mihaela van der Schaar, editors, *Proceedings of AAAI Spring Symposium on Survival Prediction - Algorithms, Challenges, and Applications 2021*, volume 146 of *Proceedings of Machine Learning Research*, pages 184–193. PMLR, 22–24 Mar 2021. URL <https://proceedings.mlr.press/v146/nagpal21a.html>.
- [22] Chirag Nagpal, Xinyu Li, and Artur Dubrawski. Deep survival machines: Fully parametric survival regression and representation learning for censored data with competing risks. *IEEE Journal of Biomedical and Health Informatics*, 25(8):3163, August 2021.
- [23] Kai Ren, Jie Qin, Liang Zheng, Zhiyuan Yang, Weinan Zhang, Lin Qiu, and Yong Yu. Deep recurrent survival analysis. In *Proceedings of the AAAI Conference on Artificial Intelligence*, volume 33, pages 4798–4805, 2019. doi: 10.1609/aaai.v33i01.33014798.
- [24] Abhinav Saxena, Kai Goebel, Dan Simon, and Neil Eklund. Damage propagation modeling for aircraft engine run-to-failure simulation. In *2008 International Conference on Prognostics and Health Management*, pages 1–9. IEEE, 2008.
- [25] Richard S Sutton. Learning to predict by the methods of temporal differences. *Machine learning*, 3(1):9–44, 1988.
- [26] Ashish Vaswani, Noam Shazeer, Niki Parmar, Jakob Uszkoreit, Llion Jones, Aidan N Gomez, Łukasz Kaiser, and Illia Polosukhin. Attention is all you need. In *Advances in Neural Information Processing Systems (NeurIPS)*, 2017.
- [27] Andre Vauvelle, Benjamin Wild, Roland Eils, and Spiros Denaxas. Differentiable sorting for censored time-to-event data. In *Thirty-seventh Conference on Neural Information Processing Systems*, 2023. URL <https://openreview.net/forum?id=gYwJI7wLhc>.
- [28] Christopher JCH Watkins and Peter Dayan. Q-learning. *Machine Learning*, 8(3-4):279–292, 1992.
- [29] Ruofan Wu, Jiawei Qiao, Mingzhe Wu, Wen Yu, Ming Zheng, Tengfei Liu, Tianyi Zhang, and Weiqiang Wang. Neural frailty machine: Beyond proportional hazard assumption in neural survival regressions. In *37th Conference on Neural Information Processing Systems (NeurIPS 2023)*, 2023.

## A Ablation study on $\tau$

The goal of this section is to study the effect of the target learning rate  $\tau$  in the variability of the estimates, and to provide empirical evidence of the stabilizing capabilities introduced by the target network. Furthermore, we also investigate the effect of different target learning rates on the performance of the models in terms of CI and IBS, demonstrating the benefits of less frequent updates of the pseudo-targets, as introduced by our framework.

We follow the same experimental setup as in Section 5.2, using three Gaussian random walk datasets with different horizons. Specifically, we generated three 20-dimensional random walk datasets as described in Section 5.1 with horizons  $H = 30$ ,  $H = 50$  and  $H = 100$ . All datasets have approximately 20% of censored sequences.

For all datasets, we fix  $\lambda = 0$  and train models for values of  $\tau \in \{0.01, 0.05, 0.1, 0.25, 0.5, 1.0\}$ . For each horizon and value of  $\tau$  we fit models on five training sets, each randomly generated with a different seed, with a size of 50. Training was conducted for 100 epochs using the same architecture and hyperparameters as described in Section 5.2 for LargeRW. Results were collected on a separate test set of size 1000 for all models.

For each sequence in the test set we collect the estimated hazard probabilities  $h_{k\ell} = h_{\theta}(k|x_{\ell})$  for  $k = 1, \dots, t$  and  $\ell = 1, \dots, t$  obtained by each model. We then calculate the mean and standard deviation of the obtained hazard probabilities,  $\bar{h}_{k\ell}$  and  $\Delta h_{k\ell}$  respectively. To obtain the variability of the estimates we re-scale the standard deviations using the variance of the Bernoulli distribution with parameter  $\bar{h}_{k\ell}$ . This re-scaling has the purpose of ‘‘canceling out’’ the inherent variability of the hazard distribution. That is, we calculate the variability of the estimations as

$$\delta_{k\ell} = \frac{\Delta h_{k\ell}}{\bar{h}_{k\ell}(1 - \bar{h}_{k\ell})}.$$

In Figure 2 we present kernel density plots of the variability of the estimates  $\delta$  over the test set for the different values of  $\tau$  and datasets with horizons  $H = 30, 50, 100$ . We observe that in all cases, for larger values of  $\tau$ , the variability of the estimates increases. This indicates that less frequent updates of the pseudo-targets introduced by the target network reduces the variability of the estimates, thus stabilizing the training procedure.

We also present the average performance of the models on the test set for the different values of  $\tau$  in Figure 3 for all datasets. In all cases we observe that both scores improve with larger values of  $\tau$ , as long as  $\tau < 1$ , which corresponds to less frequent updates of the pseudo-targets. This contrasts with the TCSR method by [16] which updates the pseudo-targets at each iteration. More specifically, for the horizon  $H = 30$  the best scores, both in terms of CI and IBS, are achieved with  $\tau = 0.1$ . Similarly, for  $H = 50$  and  $H = 100$ ,  $\tau = 0.25$  yields the best results for both metrics.

## B Further Details of TCSR

In Table 2 we summarize the main hyperparameters of the SA baselines with and without landmarking, and for the TCSR and DeepTCSR algorithms.

Table 2: Comparison of main hyperparameters of each algorithm.

ALGORITHM	$\ell$ IN MLE	$\lambda$	$\tau$	BATCH?
SA INIT ST.	0	–	–	✓
SA LANDM.	$> 0$	1	–	✓
TCSR	$> 0$	$\in [0, 1]$	–	×
DEEPTCSR	$> 0$	$\in [0, 1]$	$\in (0, 1)$	✓

## C Statistics of Datasets

The following table summarizes the statistics of the datasets used in the experimental section.

Table 3: Statistics of small datasets described in Section 5.1 and larger datasets described in Section 5.2.

DATASET	SIZE	#STATIC	#TIME-VAR.	$H$
PBC2	312	3	12	16
AIDS	467	4	1	5
SMALLRW	–	0	20	11
LARGERW	10K	0	50	100
MONLASTFM	992	0	12	53
DAYLASTFM	992	0	12	1457
NASA	200	0	16	361

Table 4: Hyperparameters details for large datasets.

Hyperparameter	MonLastFM	DayLastFM	LargeRW	NASA
Nb. layers	1	1	1	1
Hidden size	16	16	16	16
Learning rate	0.01	0.01	0.01	0.01
Nb. epochs	100	100	100	100
Dropout	0.2	0.05	0.2	0.2
Batch size	128	128	128	32

## D Further experimental details

### D.1 Evaluation Metrics

We use two standard scores for evaluating survival models, namely the Concordance Index (CI) and Integrated Brier Score (IBS).

The CI measures how well the model ranks subjects according to their survival time. It is defined as follows:

$$CI(\mathcal{D}) = P\{S(t^{(i)}|x_0^{(i)}) > S(t^{(j)}|x_0^{(j)}) : t^{(i)} > t^{(j)}\}.$$

A CI close to 1 indicates that the model captures the right order in which the subjects reach the terminal state or censoring time. In contrast, a CI close to 0.5 suggests the model is not better than a random ranking.

Another popular metric to assess survival models is the IBS, which measures the overall performance of the model across a specific time horizon. The IBS is calculated by averaging the Brier Score over time. Given a dataset  $\mathcal{D}$  the Brier Score (BS) is defined as

$$BS(k; \mathcal{D}) = \sum_{i=1}^n \left[ \frac{S(k|x_0^{(i)})^2}{\text{km}(t^{(i)})} \mathbf{1}\{k \leq t^{(i)} \wedge \neg c^{(i)}\} + \frac{(1 - S(k|x_0^{(i)}))^2}{\text{km}(k)} \mathbf{1}\{k > t^{(i)}\} \right].$$

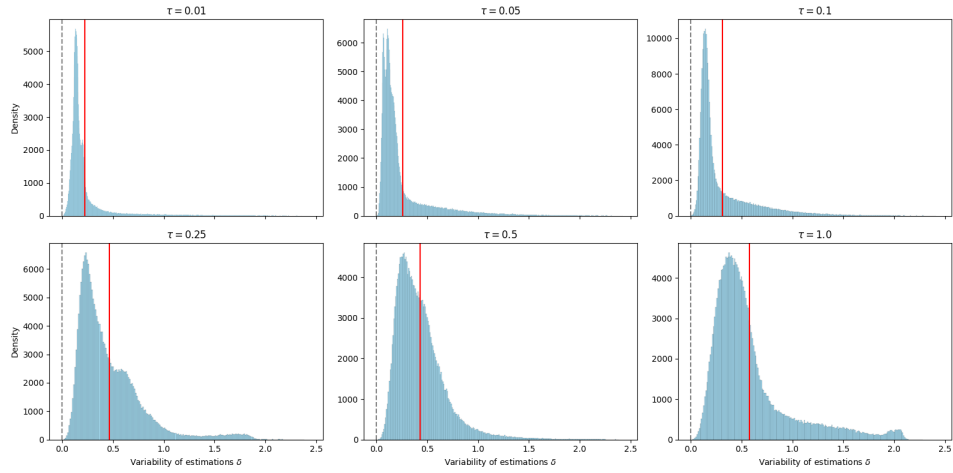
where km is the Kaplan–Meier estimator.

The BS is an error score that measures the discrepancy between the estimated survival probability and the true survival outcome. Integrating Equation (D.1) over the time gives the IBS:

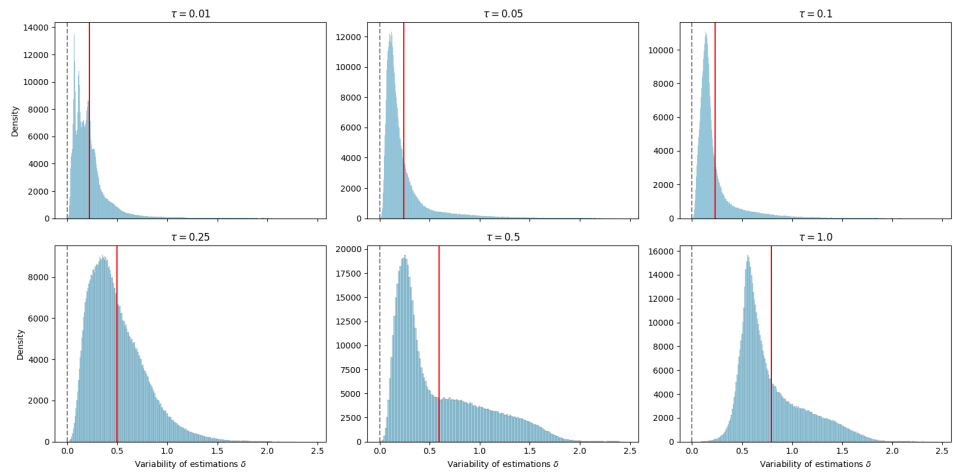
$$IBS(\mathcal{D}) = \frac{1}{H} \sum_{k=0}^{H-1} BS(k; \mathcal{D}).$$

### D.2 Architecture details

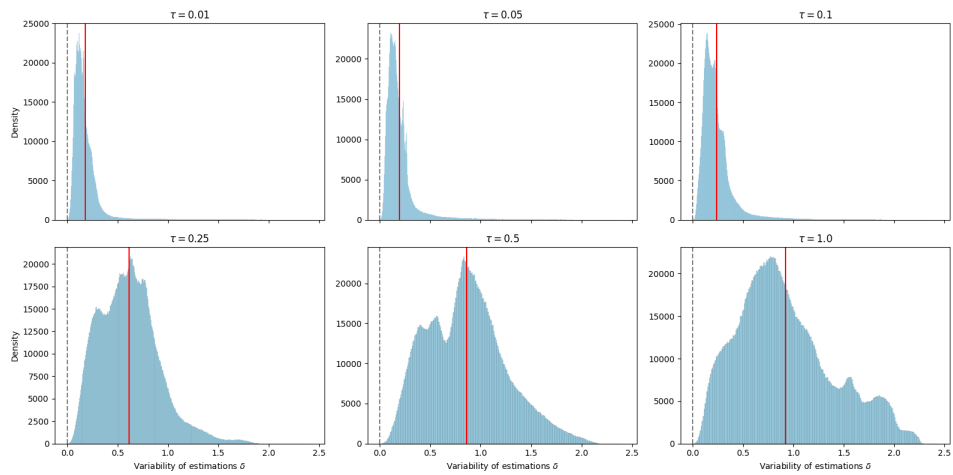
We provide further details on the architecture utilized in Section 5.2. For all datasets we fitted a single-layer transformer model. Table 4 provides all the details.



(a)

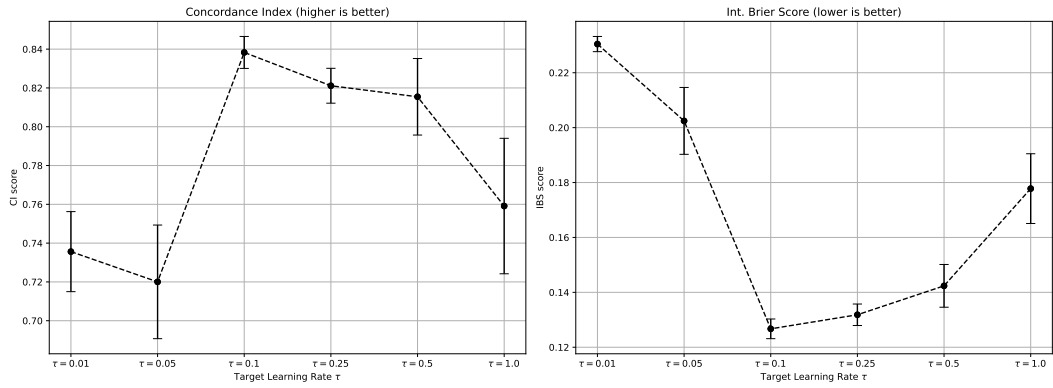


(b)

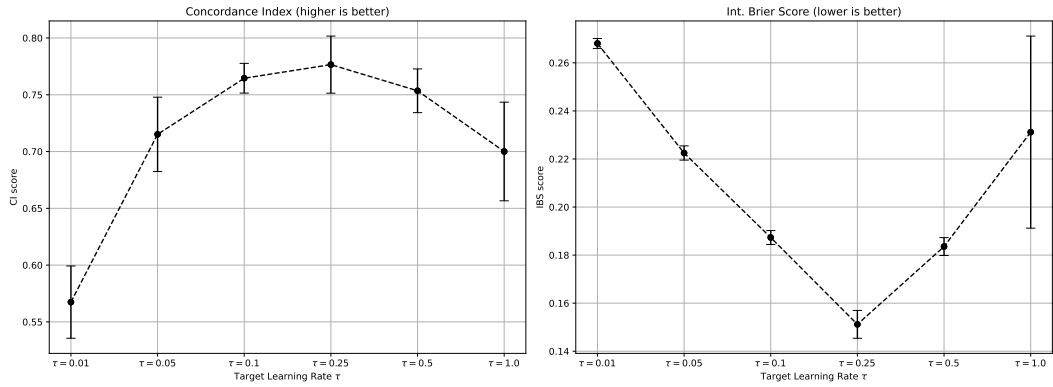


(c)

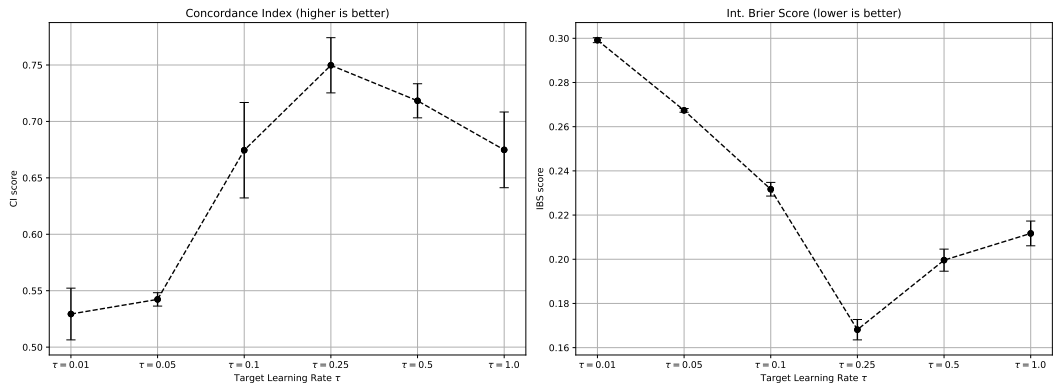
Figure 2: Variability of estimates for different values of  $\tau$  with  $\lambda = 0$  for datasets with varying horizons: (a)  $H = 30$ , (b)  $H = 50$ , and (c)  $H = 100$ . The red line indicates the mean value.



(a)



(b)



(c)

Figure 3: Concordance Index (left, higher is better) and Integrated Brier Score (right, lower is better) on the test set across five random splits for different values of  $\tau$ ,  $\lambda = 0$ , and dataset horizons: (a)  $H = 30$ , (b)  $H = 50$ , and (c)  $H = 100$ .